

# Phase-sensitive detection of Bragg scattering at 1D optical lattices

S. Slama, C. von Cube, B. Deh, A. Ludewig, C. Zimmermann, and Ph.W. Courteille

*Physikalisches Institut, Eberhard-Karls-Universität Tübingen,*

*Auf der Morgenstelle 14, D-72076 Tübingen, Germany*

(Dated: August 18, 2018)

We report on the observation of Bragg scattering at 1D atomic lattices. Cold atoms are confined by optical dipole forces at the antinodes of a standing wave generated by the two counter-propagating modes of a laser-driven high-finesse ring cavity. By heterodyning the Bragg-scattered light with a reference beam, we obtain detailed information on phase shifts imparted by the Bragg scattering process. Being deep in the Lamb-Dicke regime, the scattered light is not broadened by the motion of individual atoms. In contrast, we have detected signatures of global translatory motion of the atomic grating.

PACS numbers: 42.50.Vk, 05.45.Xt, 05.65+b, 05.70.Fh

Elastic Rayleigh scattering is a phase-coherent process. In thermal atomic clouds however the photonic recoil transferred to the atoms by the scattering process introduces inhomogeneous line broadening washing out the phase-coherence. Furthermore, Rayleigh scattering only dominates at small intensities; stronger pumping causes power broadening, which merely increases the inelastic components of the resonance fluorescence. For these reasons it is difficult to directly measure the phase-shift induced by Rayleigh scattering.

A phase-coherent study of Rayleigh scattering is facilitated by two measures: 1. Using cold and strongly confined atoms, and 2. arranging for long-range order in the atomic cloud. By cooling the atoms the Doppler-broadening is reduced; by tightly confining them within a very small region of space, i.e. within the Lamb-Dicke limit, no recoil is imparted to individual atoms; and by creating density gratings the elastic part of the resonance fluorescence is concentrated into a very small solid angle. The resonant enhancement of the structure factor for elastic Rayleigh scattering by atomic long-range order is called Bragg scattering.

Periodic structures are generally probed by Bragg scattering. A probe beam is shone onto the sample under a certain angle, the so-called Bragg angle, and the emergence of phase-coherent light at well-defined sharp solid angles is a signature of long-range order. This procedure can be applied to periodic arrangements of atoms in optical gratings. Bragg scattering of light at 3D atomic lattices has for the first time been observed by Birkel *et al.* and Weidemüller *et al.* [1, 2].

The elastic peak of the atomic response to incident laser light has been observed in several experiments. Westbrook *et al.* [3, 4] used the heterodyne method to beat down the fluorescence of magneto-optically trapped atoms with a local oscillator to electronically accessible frequencies. It is in principle possible to probe the *complete* fluorescence spectrum, i.e. the Mollow triplet and the elastic Rayleigh peak by scanning the reference laser. This technique permitted Westbrook *et al.* to de-

tect Dicke-narrowing of Rayleigh scattering in magneto-optical traps. However in this experiment the heterodyne signal was integrated over long times, so that the phase-coherence of the elastic scattering process is not directly shown.

We report here the first detailed phase information of the Rayleigh scattering process. The progress was possible by combining the techniques of heterodyning and Bragg scattering. In contrast to previous experiments, we exploit the heterodyne technique interferometrically: The frequency beat between the Bragg reflected light and a reference laser having a different frequency is demodulated. From the two quadrature phases, we completely recover the complex scattering coefficient. We ramp the frequencies of both laser beams, the Bragg beam and the reference beam simultaneously, so that the beat frequency is fixed. Because the elastically scattered light is always phase-coherent, we can look for phase shifts due to the scattering process. When we ramp the laser frequencies, we basically probe the resonant enhancement of the Rayleigh peak close to the Bragg condition. At the same time our experiment represents the first observation of Bragg scattering at 1D atomic density gratings. With a Lamb-Dicke factor on the order of 100 we are deep in the Lamb-Dicke regime.

The optical layout of our experiment is shown in Fig. 1. It consists of a high-finesse ring cavity, which has been discussed in Ref. [5] and a setup for Bragg scattering. The ring cavity has a finesse of 80000 and a waist of  $w_{dip} = 130 \mu\text{m}$ . From a titanium-sapphire laser operating at  $\lambda_{dip} = 796 - 820 \text{ nm}$  two light frequencies  $\omega_{\pm}$  are generated by means of acousto-optic modulators (AOM). The light beams pump the two counter-propagating modes of the ring cavity near resonance, thus forming a standing wave, which propagates at a velocity  $v$  given by  $2k_{dip}v = \omega_{+} - \omega_{-}$ . The intracavity power is  $P_{cav} = 1 - 10 \text{ W}$ . Typically  $N_{tot} = 10^7$   $^{85}\text{Rb}$  atoms are loaded from a standard magneto-optical (MOT) trap into the standing wave, which is red-detuned with respect to the rubidium  $D_1$  line. Typically the temperature of the

cloud is on the order of few 100  $\mu\text{K}$ .

The light of a blue laser diode (Toptica LD-0405-0005-2) operating at  $\lambda_{brg} = 420.2$  nm is split into a probe beam,  $\omega_i$ , and a reference beam  $\omega_r$ . The frequencies of the beams are controlled by means of AOMs. Some time after loading the atoms into the standing wave, the light beam  $\omega_i$  is pulsed and shone under an angle of  $\beta_i = 58^\circ$  onto the atoms. The light reflected from the atoms,  $\omega_s$ , is detected under the angle  $\beta_s = -\beta_i$  with a photomultiplier (PMT) (Hamamatsu 1P28) terminated with a resistive load of  $R = 100$  kHz. Some experiments were performed by carefully phase-matching the Bragg beam with a reference beam  $\omega_r$  (then the shutter  $S$  is open). In this case, the PMT signal was amplified with a transimpedance amplifier (FEMTO DHPCA-200).

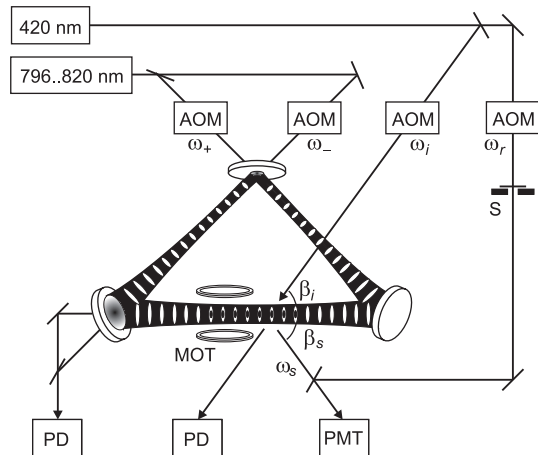


FIG. 1: The experimental setup consists of a ring cavity pumped at 796 - 820 nm and a diode laser at 420 nm for Bragg scattering. The shutter  $S$  controls the reference beam used to detect frequency beats between the Bragg and the reference beam.

Our standing wave dipole trap represents a 1D optical lattice, whose periodicity is  $\frac{1}{2}\lambda_{dip} = \pi/k_{dip}$ . The Bragg condition requires  $\lambda_{dip} \cos \beta_i = \lambda_{brg}$ . To resonantly enhance the Bragg scattering, which otherwise would be negligibly small, we tune the laser to the transition  $5S_{1/2}, F = 3 \rightarrow 6P_{3/2}, F' = 2, 3, 4$  with a natural linewidth of  $\Gamma_{brg}/2\pi = 1.3$  MHz [6]. During the Bragg pulse sequence the repumping laser of the magneto-optical trap is shone onto the atoms to minimize optical pumping into the ground state  $F = 2$  level.

The efficiency of Bragg scattering depends critically on the angle of incidence  $\beta_i$ : The acceptance angle is about  $0.1^\circ$ . The scattered light beam has a nearly Gaussian elliptical shape. It is collimated in the scattering plane having about the same diameter as the input beam  $w_z = 250$   $\mu\text{m}$ . This means that about  $N_s \simeq 630$  planes of the atomic lattice are illuminated, the lattice itself being longer. Therefore only a small fraction,  $N \simeq N_{tot}/16$ , of the atoms confined in the dipole trap are illuminated

by the Bragg beam. The radial size of the atomic cloud,  $w_r \approx 30$   $\mu\text{m}$ , determines the scattered beam divergence in the direction orthogonal to the scattering plane. We calculate the solid angle  $d\Omega_s$  in the far field, where both beams are divergent and the grating can be considered a point source as  $\Omega_s \equiv 2\lambda_{brg}^2/\pi w_r w_z \approx 1.5 \times 10^{-5}$ .

The power  $P_s$  diffracted by Bragg scattering into a direction  $d\Omega_s$  can be estimated from [6]:

$$\frac{dP_s}{d\Omega_s} = I_i \frac{\pi^2}{\lambda_{brg}^4} \left| \frac{\alpha}{\epsilon_0} \right|^2 \sin^2 \xi \left| \sum_m e^{i\Delta\mathbf{k}\mathbf{R}_m} \right|^2 f_{DW}^2, \quad (1)$$

where

$$\alpha = \frac{6\pi\epsilon_0}{k_{brg}^3} \frac{\Gamma_{brg}}{2\Delta_{brg} + i\Gamma_{brg}} \quad (2)$$

is the frequency-dependent complex polarizability.  $\Delta_{brg}$  is the Bragg laser detuning. We actually use  $I_i = 1$  mW/cm<sup>2</sup> incident intensity, which is about half the saturation intensity  $I_s$  and corresponds to the power  $P_i = \frac{\pi}{2} w_z^2 I_i \approx 1$   $\mu\text{W}$ . The sum over individual atoms represents the structure factor,  $\sum_m e^{i\Delta\mathbf{k}\mathbf{R}_m} = \sum_m e^{i2mk_{brg}\lambda_{dip} \cos \beta} = N_s$ . The Bragg scattered light power is proportional to the square of the atom number as is verified in Fig. 2(a).

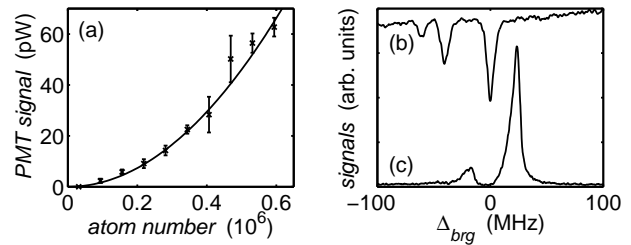


FIG. 2: (a) The quadratic dependence of the Bragg scattered power  $P_s$  on the atom number  $N$  agrees well with Eq. (1). (b) Absorption spectrum of magneto-optically trapped atoms showing the hyperfine levels  $F' = 2, 3, 4$ . (c) Bragg reflection spectrum obtained by ramping the blue laser frequency. Here the shutter  $S$  in Fig. 1 blocked the reference beam. Only the two strongest hyperfine peaks are visible.

The Debye-Waller factor is given by  $f_{DW} = \overline{e^{i\Delta\mathbf{k}\mathbf{x}}} = e^{-\frac{1}{2}(\Delta k_z)^2 \bar{z}^2}$ , since only the distribution of atoms along the lattice normal axis  $\hat{z}$  contributes to the Debye-Waller factor,  $\Delta k_{x,y} = 0$  and  $\Delta k_z = 2k_{brg} \cos \beta_i$ . The rms-size of the atomic cloud is  $\bar{z} = k_{dip}^{-1} \sqrt{k_B T / 2U_0}$  in the harmonic approximation of the trapping potential. We noticed in earlier experiments [5, 7] that the temperature of the cloud tends to adopt a fixed ratio with the depth of the dipole trap,  $T \approx 0.2 U_0$ . Therefore, the spatial distribution of the atoms (and thus the Debye-Waller factor) does not vary much with temperature, so that we estimate  $f_{DW} = 0.8$ . Finally,  $\xi$  is the angle between the polarization of the incident light and the diffracted

wavevector. In our case, since the incident light is  $p$ -polarised with respect to the atomic grating,  $\xi = 90^\circ$ . With the above estimations we calculate for the scattered power on resonance from Eq. (1)  $P_s \approx 400$  nW.

Fig. 2(c) shows a spectrum of the Bragg resonance obtained by ramping the laser frequency at 420 nm (with the shutter  $S$  closed and  $\omega_+ = \omega_-$ ). Three hyperfine components are expected in the spectrum, i.e.  $F' = 2, 3, 4$ . However, the  $F' = 2$  component is too weak to be seen. The other lines have a relative line strength of 1 : 3 and are separated by 40 MHz. Fig. 2(b) shows a MOT absorption spectrum for reference. The frequency displacement between the spectra is due to the light shift of the atoms in the dipole trap.

The measured peak intensity of the Bragg reflected light is on the order of  $\tilde{P}_s = 100$  pW. During a scan the laser is swept over the resonance within a time of  $\Delta t = 1$  ms, which is sufficient to scatter about  $\Delta t P_s / 2\hbar\omega_s \approx 200\,000$  photons. Defining the reflectivity as the ratio of the scattered power and the fraction of power incident on the atoms (i.e. reduced in order to account for the partial overlap between the incident beam and the atomic cloud),  $R = \tilde{P}_s / (\frac{1}{2}\pi w_r w_z I_i)$ , we obtain for the amplitude reflection coefficient,  $|r| = \sqrt{R} \approx 3\%$ .

The discrepancy between the calculated and the measured Bragg-reflected power, which has also been observed in [2], is due to a combination of two effects: First, the dipole-trapped atoms are subject to a position-dependent Stark shift, which inhomogeneously broadens the Bragg spectrum. This effect, which depends on the potential depth  $U_0$  and the temperature  $T$ , leads to asymmetric resonance peaks, as seen in Fig. 2(c). From calculations we estimate a line broadening of about  $10\Gamma_{brg}$  resulting in a strong reduction of the Bragg-reflected light peak intensity. Second, incoherent processes occur at a rate of  $(I_i/I_s) (1 + 4\Delta_{brg}^2/\Gamma_{brg}^2)^{-1} \lesssim 0.5$  times the elastic scattering rate. These processes cause heating and optical hyperfine pumping. In fact, we observe noticeable depletion of the lattice when scanning the blue laser over the resonance. Experimentally, we reduce the light power and increase the scanning speed to avoid distortion of the line profile due to heating during a scan.

The spectroscopy detailed above only yields the absolute value of the reflection coefficient  $|r|$ . To also measure its phase, we phase-match the Bragg beam with a reference laser beam and observe the frequency beat on the PMT signal. By passing the beam shone onto the atomic cloud,  $\omega_i$ , and the reference beam,  $\omega_r$ , through acousto-optic modulators (see Fig. 1), we can arbitrarily choose the beat frequency. We expect to see the frequency component  $\Delta\omega_i \equiv \omega_i - \omega_r$  in the beat signal. A typical spectrum is shown in Fig. 3(a).

Laser frequency fluctuations limit the resolution of the spectrum. On a long time-scale the laser emission bandwidth is estimated to be less than 5 MHz. However, the time-scale on which the spectrum is recorded (a few milli-

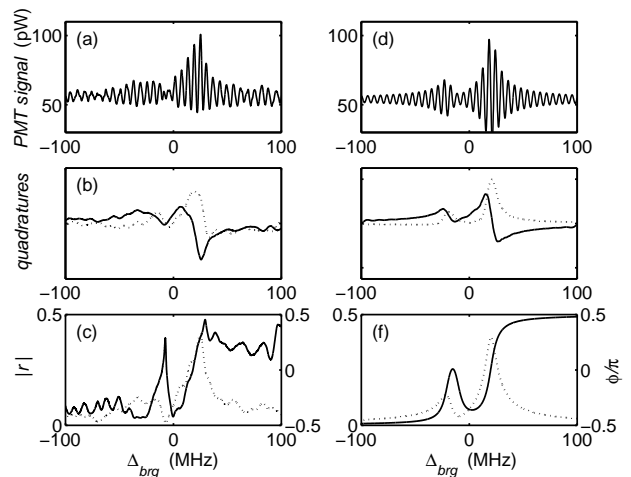


FIG. 3: (a) Beat signal recorded while tuning the blue laser across resonance. The frequencies were chosen such that  $\Delta_i = (2\pi)5.4$  kHz. (b) Quadrature components of the beat signal and (c) amplitude profile calculated from the quadrature components and phase profile as obtained by counting the number of oscillations in Fig. (a) per time interval. (d) Simulated beat signal spectrum between Bragg-scattered light and a reference beam using a calculated amplitude and phase profile. (e) Quadrature components of the Bragg beat demodulated with the reference beat. (f) Amplitude (dashed) and phase profile (solid) as derived from the quadrature components. The profiles coincide with the profiles used to calculate the curves in Fig. (d).

seconds) is so short, that acoustic noise does not completely inhibit phase-sensitive detection.

When light is scattered at an unbound atomic cloud, the elastic Rayleigh peak is Doppler-broadened by the recoil imparted to the atoms, whose velocities have a Maxwell-Boltzmann distribution. However in axial direction the atoms are localized to less than  $\lambda_{dip}/2 \ll \lambda_{brg}$ , so that the resonance fluorescence spectrum is Dicke-narrowed. The rate of inelastic scattering events in which the vibrational quantum number changes, is reduced by the Lamb-Dicke factor  $(2n_z + 1)\epsilon/\Omega_z \approx 0.01$ , where  $n_z$  is the vibrational quantum number for axial atomic oscillation,  $\Omega_z$  the oscillation frequency and  $\epsilon$  is the recoil frequency. Elastic scattering events involving no change in vibrational level are favored. The spectrum is thus Doppler-free, and we do not expect recoil shifts.

The complex scattering amplitude  $r = |r|e^{i\phi}$  represents the global response of the atomic cloud to an incident laser  $E_i = E_{i0}e^{i\omega_i t}$ . Thus the Bragg scattered light is given by  $E_s = rE_i = |r|E_{i0}e^{i\omega_i t + i\phi}$ . While the amplitude  $|r|$  is obtained via simple absorption spectroscopy, acquiring phase information  $\phi(t)$  needs heterodyning. Therefore we beat the Bragg scattered light with a reference beam  $E_r = E_{r0}e^{i\omega_r t}$  while scanning over the resonance,  $I = |E_r + E_s|^2$ . We obtain  $I \approx E_{r0}^2 + |r|^2 E_{i0}^2 + 2|r|E_{r0}E_{i0} \cos(\Delta\omega_i t + \phi)$ .

In order to extract amplitude and phase from a beat signal spectrum shown in Fig. 3(a), we extract the quadrature and the in-phase component by numerically demodulating the beat signal with  $\cos \Delta\omega_i t$  and  $\sin \Delta\omega_i t$ . Low-pass filtering the DC components in the Fourier spectrum yields  $\bar{U}_s = -|r|E_{r0}E_{i0} \sin \phi$  and  $\bar{U}_c = |r|E_{r0}E_{i0} \cos \phi$ . Fig. 3(b) shows the quadrature phases. Phase and amplitude follow from  $rE_{r0}E_{i0}(t) = (\bar{U}_c^2 + \bar{U}_s^2)^{1/2}$  and  $\tan \phi(t) = -\bar{U}_s/\bar{U}_c$ . The result is shown in Fig. 3(c). We notice an absorptive profile for the reflection amplitude, which coincides with the profile recorded without heterodyning (shutter  $S$  is closed) [see Fig. 2(c)]. The dispersively shaped phase profile in Fig. 2(c) exhibits a maximum phase shift on the order of  $\pi$  and a distortion due to the hyperfine splitting of the upper level.

To describe the observation we calculate the complex reflection coefficient  $r \propto \alpha$  based on the evaluations accompanying Eq. (1) and use it to generate the beat signal shown in Fig. 3(d). This signal, if submitted to the same data processing as for the experimental data, yields the curves in Figs. 3(e-f). In particular, the amplitude and phase profile of Fig. 3(f) exactly recover the calculated complex reflection coefficient. To compare with the experiment, we adjust the power values in the modes  $E_r \approx E_i \approx 54$  pW. We notice a good agreement, despite the noise appearing in the measured data. This noise is due to frequency fluctuations of the blue laser beam and to variations in the position of the ring cavity standing wave.

The phase delay is intrinsically connected with the Rayleigh scattering process, which predicts a phase shift described by  $\tan \phi = \text{Im } \alpha / \text{Re } \alpha = -\Gamma_{brg} / 2\Delta_{brg}$ , i.e. the phase evolves from  $\phi = 0$  to  $-\pi$  across the resonance as shown in Fig. 3(f). Additional phase shifts may, in principle, result from the finite propagation time of the incident beam slowed down by refractive index variations in the optically dense cloud, and from multiple scattering between the atomic layers. In our case, the finite radial size of the scattering layers limits the effective number of layers participating in multiple scattering to  $N_{eff} = 2w_r / \lambda_{dip} \tan \beta_i \approx 160$ . We estimate our mean density to  $n = 5 \times 10^{11} \text{ cm}^{-3}$ . In this thin grating regime, the above effects are not expected to contribute to the observed signals. We verified the validity of this assumption by calculating the complex reflection coefficient using the transfer matrix formalism for Bragg scattering developed by Deutsch *et al.* [8], and we found identical results.

Our detection method is well-suited not only to probe atomic gratings, but also to detect their "motional dynamics". To demonstrate this we let the standing wave rotate in the ring cavity with velocity  $v$  by supplying different pump frequencies,  $\omega_+ \neq \omega_-$ . Fig. 4 demonstrates that the Bragg scattered light is frequency-shifted by  $\Delta\omega_s \equiv \omega_s - \omega_r = \Delta\omega_i - 2k_{dip}v$ . The asymmetric broadening of the Fourier spectrum of the Bragg beat in Fig. 4(c) arises from the fact that the beat signal, being a

scan over two hyperfine resonances, is non-periodic. The carrier frequency corresponds to the rightmost peak of the spectrum.

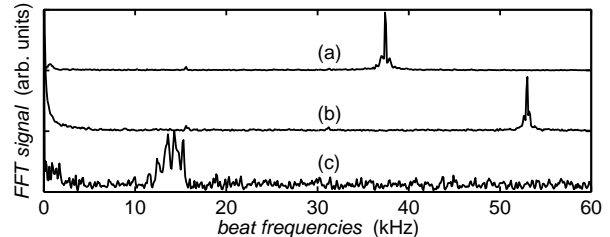


FIG. 4: Detection of moving Bragg lattices. Shown are the Fourier spectra of (a) the Doppler-shift  $2k_{dip}v = \omega_+ - \omega_- = (2\pi)37$  kHz, (b) the reference interferometer  $\Delta\omega_i = (2\pi)52$  kHz and (c) the Bragg interferometer  $\Delta\omega_s = (2\pi)15$  kHz.

In conclusion, periodic ordering in atomic clouds can have dramatic influence on the propagation and scattering of light. For thin atomic lattices, the Rayleigh scattered light destructively interferes in all but one direction. The resonant enhancement of Rayleigh scattering in this direction provided us with enough intensity to realize a "Bragg interferometer" in an atomic gas. This method may prove sufficiently accurate for probing interesting features of Bragg scattering in the limit where multiple reflections between adjacent layers are frequent, such as the occurrence of photonic band-gaps for certain ranges of light detuning or incident angle [8].

Long-range order does not need to be created by periodic force fields. Under certain circumstances [9] atomic ensembles driven by dissipative forces spontaneously arrange themselves into propagating periodic lattices. An interesting application of our method of detecting moving lattices could be the study of the bunching of such systems.

We acknowledge financial support from the Landestiftung Baden-Württemberg.

- 
- [1] G. Birkl *et al.*, Phys. Rev. Lett. **75**, 2823 (1995).
  - [2] M. Weidemüller *et al.*, Phys. Rev. Lett. **75**, 4583 (1995).
  - [3] C. I. Westbrook *et al.*, Phys. Rev. Lett. **65**, 33 (1990).
  - [4] P. Jessen *et al.*, Phys. Rev. Lett. **69**, 49 (1992).
  - [5] D. Kruse *et al.*, Phys. Rev. A **67**, 51802(R) (2003).
  - [6] M. Weidemüller, A. Görlitz, Th. W. Hänsch, and A. Hemmerich, Phys. Rev. A **58**, 4647 (1998).
  - [7] B. Nagorny *et al.*, Phys. Rev. A **67**, 31401(R) (2003).
  - [8] I. H. Deutsch, R. J. C. Spreeuw, S. L. Rolston, and W. D. Phillips, Phys. Rev. A **52**, 1394 (1995).
  - [9] D. Kruse, C. von Cube, C. Zimmermann, and Ph. W. Courteille, Phys. Rev. Lett. **91**, 183601 (2003).